Velocity Overshoot Effects and Scaling Issues in III–V Nitrides

Madhusudan Singh, *Student Member, IEEE*, Yuh-Renn Wu, *Student Member, IEEE*, and Jasprit Singh

***Abstract*—Empirical evidence from submicrometer technology in GaAs- and InGaAs-based field-effect transistors (FETs) has led to an expectation that velocities exceeding the steady state values would be observed in III–V nitride devices. However, scaling of devices down to 0.7 and 0.25 μm has so far not yielded any performance enhancement that may suggest an overshoot. In this paper, we examine transport in AlGaN–GaN heterojunction FETs (HFETs) to examine whether velocity overshoot effects occur. Our findings show that very high scattering rates when combined with unusual field profiles, result in a change in the local transport mechanism, and, in the source-gate region, combine to reduce/nullify velocity overshoot effects. We also find that the effect of nonequilibrium phonons on transport in the channel is minimal, with the peak nonequilibrium phonon occupation being smaller than the equilibrium phonon occupation.**

***Index Terms*—III–V nitrides, field reversal, nonequilibrium phonons, self-heating, transport mechanism, velocity overshoot.**

I. Introduction

IT IS WELL known that in submicrometer field-effect transistors (FETs) made from small effective mass materials like GaAs and InGaAs, velocity overshoot effects play a dominant role [1]. This is borne out by higher performance for submicrometer devices than is expected from simple steady-state velocity models. In the case of AlGaN–GaN HFETs, a few experimental results that are available have shown trends that suggest that velocities in the GaN channel do not exhibit overshoot effects (a few electro-absorption measurements [2] indicate an initial overshoot but the velocity does not overshoot over the entire channel). This paper addresses the following issues. 1) Does velocity overshoot occur in submicrometer AlGaN–GaN HFETs? 2) Does velocity overshoot lower the overall transit time in the channel? 3) What are the inherent sources of differences in transport in low effective mass device channels and III–V nitride based channels?

We consider a device structure schematically represented in Fig. 1 with the geometry and composition described in the caption. The structure, as suggested by the figure, is not self-aligned.

II. Formalism

The spatial dependence of electric field in the HFET is also of great importance in understanding transport in submicrometer devices. We use the finite element method to solve the two-dimensional Poisson equation and drift-diffusion equation. The Gümmel iteration method [3] is used for global convergence. Slotboom variables are used for linearizing the drift-diffusion equations. The effects of the polarization at the AlGaN/GaN interface are included through a charge control model [4], [5]. We use the steady-state velocity field curves [6] to obtain the field-dependent mobility model. This also yields the drain currents at the specified bias points. In Fig. 2, we present steady-state velocity-field curves for the device structure at $\mathrm{T} = 300$ K. The characteristics are only weakly dependent on the gate bias. A comparison with previously published work [7] indicates good agreement with the values used for comparison with experimental data.

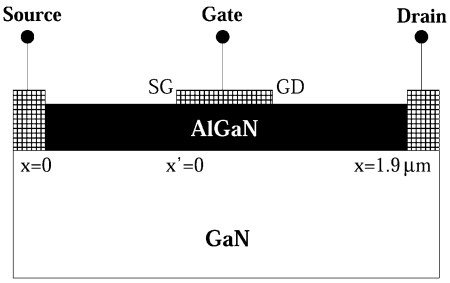

Fig. 1. Schematic (not to scale) for an AlGaN–GaN FET device structure. The $Al_{0.35}Ga_{0.65}N$ barrier layer is 290 Å thick. GaN is unintentionally doped with a gate width of 150 μm. If the source contact is presumed to lie at $x = 0$, the drain contact shown above lies at $x = 1.9$ μm. Though the precise placement of the gate depends on the gate length under consideration, the drain end of the gate (marked **GD**) lies at $x \approx 0.9$ μm in each case. The source end of the gate (marked **SG**) depends on the gate length. The origin $\mathrm{x}' = 0$ for purposes of the Monte Carlo simulations is located at this point.

The steady-state field profiles can be used to derive expected steady-state channel velocity (v_{ss}) profiles for transiting electrons

$$\begin{aligned} &(\text{ velocity-field}) f_v\colon E \mapsto v \\ &(\text{ position-field}) f_E\colon x \mapsto E \\ &(\text{ velocity}) \Rightarrow v_{\mathrm{ss}} = f_v \circ f_E \end{aligned} \tag{1}$$

where the function f_v is known from steady-state Monte Carlo simulations, and the function f_E is known from the finite element Poisson equation solver described above. It is worth mentioning here that these velocity profiles are velocity-field curves mapped on to the channel coordinate, and *not* velocity-field curves per se.

The difference between v_{ss} and the velocities obtained from the ensemble Monte Carlo calculation are indicative of whether the electron achieves overshoot over significant regions of the

Manuscript received October 21, 2004; revised December 20, 2004. This work was supported by the Office of Naval Research under Grant F004 815. The review of this paper was arranged by Editor C.-P. Lee.

The authors are with the Department of Electrical Engineering and Computer Science, The University of Michigan, Ann Arbor, MI 48109 USA.

Digital Object Identifier 10.1109/TED.2005.843966

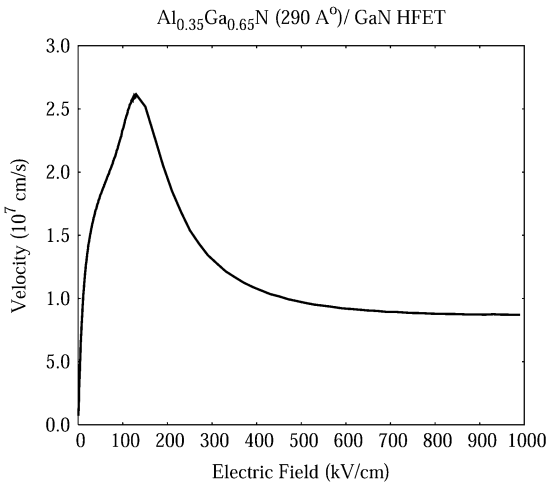

Fig. 2. Steady-state velocity-field characteristics for the $Al_{0.35}Ga_{0.65}N$ structure shown in Fig. 1 at $T = 300\ K$ and for a gate bias of 0 V.

channel. Both v_{ss} and the ensemble averaged channel velocity will be presented in the results that follow. We carry out ensemble Monte Carlo simulations with 200 000 electrons on this structure. It must be pointed out that this number corresponds to the number of electrons used in statistical averaging of calculated properties like velocity, etc. and *not* any physical density of electrons. Further, velocity overshoot is best described as nonlocal transport where the velocity of the electron at a certain point in the channel depends not only on the electric field at the point but also the history of the motion of the electron. We also examine the importance of nonequilibrium phonons as a result of phonon emission. The ensemble Monte Carlo calculation can be used in an iterative fashion.

1) Carry out ensemble simulation and keep count of number of phonons (as in Fig. 8).
2) Calculate the extra occupation of phonons corresponding to electron transit through the channel.
3) Add this extra contribution to equilibrium phonons and carry out another ensemble simulation.
4) If necessary (if the extra contribution is significant), repeat steps 1–3.

The phonon occupation at different points of the channel are estimated simply using the expression

$$\langle n(x)\rangle = G_{\rm ph}(x) \times \tau_{\rm ph} = n_{\rm ph}(x) \cdot \frac{I_{\rm ds}}{en_k} \times \tau_{\rm ph} \quad (2)$$

where $G_{\rm ph}$ is the phonon generation rate, $\tau_{\rm ph}$ is the phonon lifetime, $I_{\rm ds}$ is the drain current at the bias point (calculated using the method described earlier) and n_k is the number of κ-space modes in the device. In our paper, we have taken the phonon lifetime to be 0.3 ps, consistent with values used in literature [8].

III. Results

In all the results that follow, we assume that the device is biased with $V_{\rm ds} = 10$ V, and at 300 K, except when otherwise

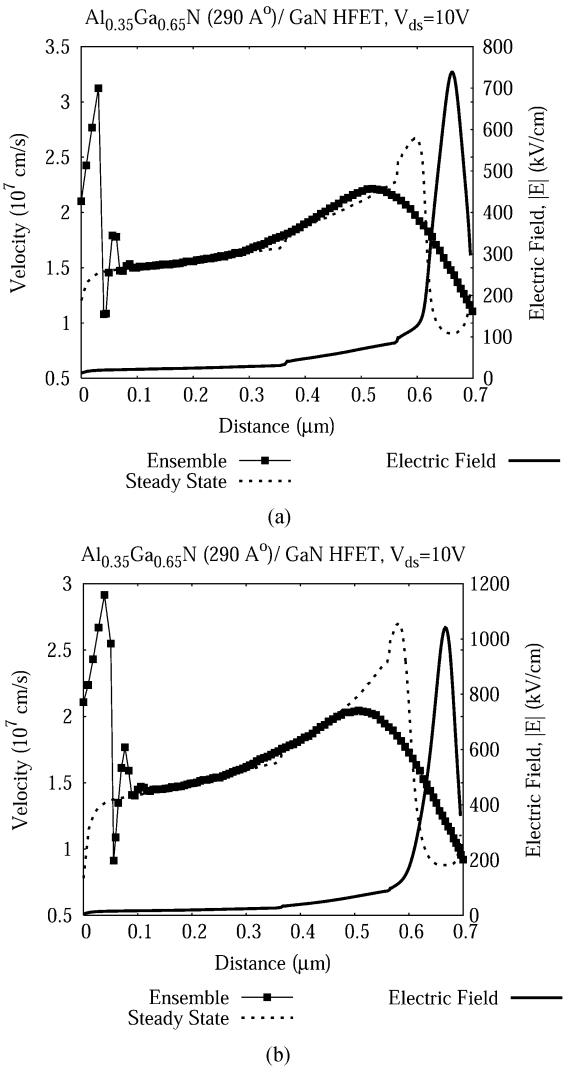

Fig. 3. $L_g = 0.70\ \mu$m. Ensemble Monte Carlo channel velocity profile, the corresponding steady-state velocity profile calculated from the velocity field relations [6], and the electric field in the channel for (a) $V_{\rm gs} = -2$ V and (b) $V_{\rm gs} = -4$ V.

stated. Further, the origin is shifted to the source end of the gate (marked **SG** in Fig. 1). At this point, carriers are assumed to be injected into the channel with thermal velocities at the temperature at which the devices are simulated. In Fig. 3, we present the results for the channel velocity profiles for $L_g = 0.7\ \mu$m. It may be noted that the velocity-field relations for AlGaN–GaN structures are well known to be nonlinear in several electric field regimes [6], [9]. The effect of this is often an inverse relationship between the steady-state velocity and the local electric field (as seen in Fig. 3 and in many of the results later). The corresponding results for $L_g = 0.25$ and $0.12\ \mu$m are shown in Figs. 4 and 5, respectively. A feature of the transport for $L_g = 0.12\ \mu$m is that the electron moves across the channel nearly ballistically.

Though the results above predict a significant overshoot for the smaller gate lengths ($L_g = 0.12, 0.25\ \mu$m), a drain bias of 10 V is probably not a practical bias [10]–[12] for usual circuit conditions for these gate lengths. The calculated electric field

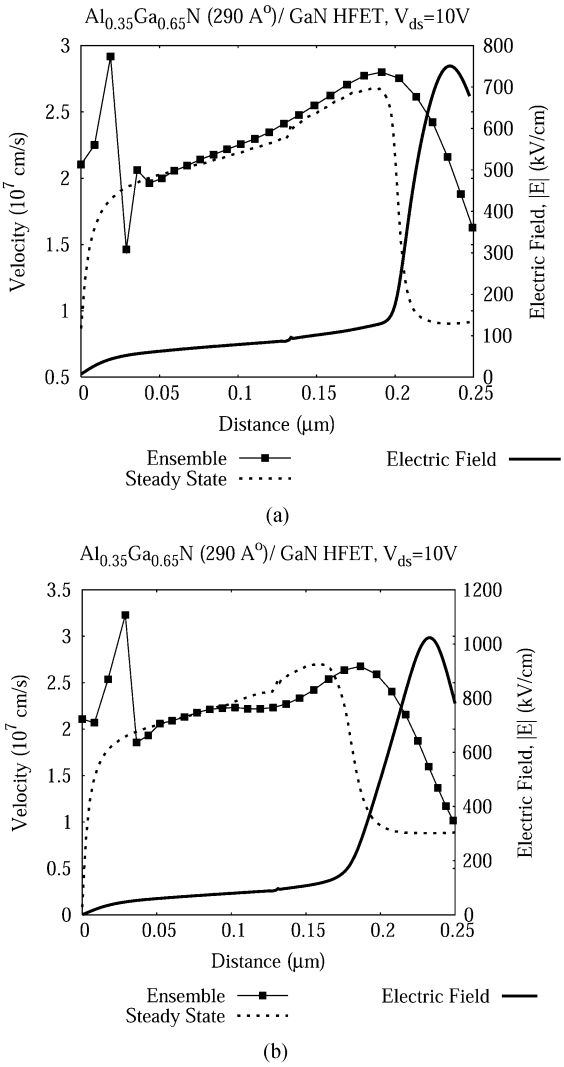

Fig. 4. Electric field and channel velocity profile results for $L_g = 0.25$ μm for (a) $V_{\rm gs} = -2$ V and (b) $V_{\rm gs} = -4$ V.

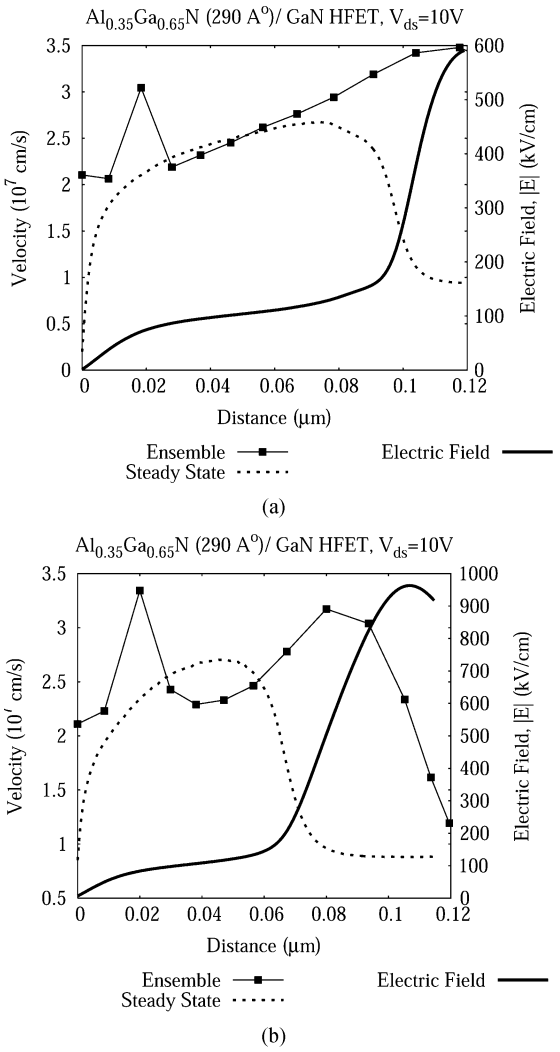

Fig. 5. Electric field and channel velocity profile results for $L_g = 0.12$ μm for (a) $V_{\rm gs} = -2$ V and (b) $V_{\rm gs} = -4$ V.

for $V_{\rm ds} = 10$ V in Figs. 4 and 5 is $\sim$1 MV/cm. To look at the results when possible device reliability concerns are not a likely issue, we also present results for a smaller drain bias (5 V) in Fig. 6. As can be seen, there is no velocity overshoot even at these small gate lengths for the lower drain bias. This is probably due to high scattering rates in the III–V nitride systems, which can be as high as 10^{14} s^{-1}.

We now examine the effect, if any, of nonequilibrium phonons in the transport. To illustrate this, we consider an extreme case: $L_g = 0.12$ μm. The device structure under consideration is a nonself-aligned structure. To better understand the process of carrier energy relaxation, we carried out a simulation that attempts to model the transport of the electron past the area described under the gate. The results for this case are shown in Fig. 7. It can be seen that the electron velocities approach about 1×10^7 cm·s^{-1}, which is close to the high field saturation velocity seen in such structures. During the ensemble simulation, a count is kept of the polar optical phonon emission events, as a function of the forward momentum ($q_{\rm par}$) and absolute value of the transverse momentum ($|q_{\rm perp}|$). Such a count is then ensemble averaged, and the result is shown in Fig. 8.

We also study the position dependence of nonequilibrium phonon generation in this system [Fig. 7(b)]. A large number of phonons are emitted outside the region under the gate, rather than under it. The equilibrium polar optical phonon occupation at 300 K is $\approx$0.03. However, the peak of the resulting phonon occupation profile in Fig. 7(b), is less than half of the equilibrium population. The extra contribution then is much less than the equilibrium phonon occupation, and as a result, these extra, nonequilibrium (or *hot*) phonons do not appear to critically affect transport in the channel. A second ensemble calculation with the updated phonon populations reveals only minor changes with respect to the channel velocity profile shown in Fig. 7(a).

Fig. 9 indicates a small but significant region of field reversal in the channel electric field profile. The reasons for this reversal are: 1) large charge gradient and 2) large change in the potential. As discussed earlier, Fig. 3 shows the channel velocity profile obtained after an ensemble Monte Carlo simulation

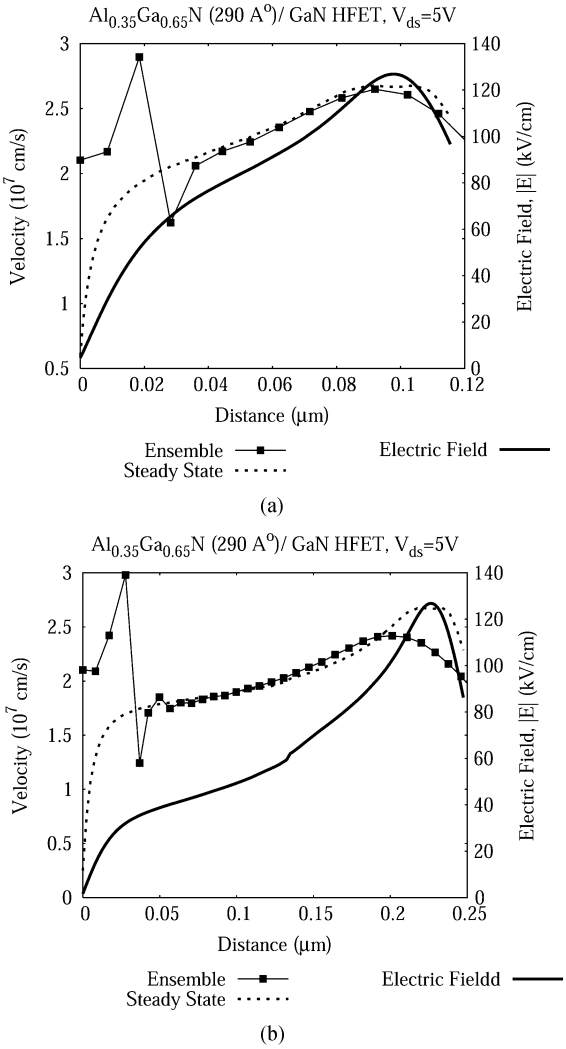

Fig. 6. Electric field and channel velocity profile results for $V_{\rm gs} = -2$ V, $V_{\rm ds} = 5$ V for (a) $L_g = 0.12$ μm and (b) $L_g = 0.25$ μm. Velocity overshoot appears to be suppressed for these bias conditions.

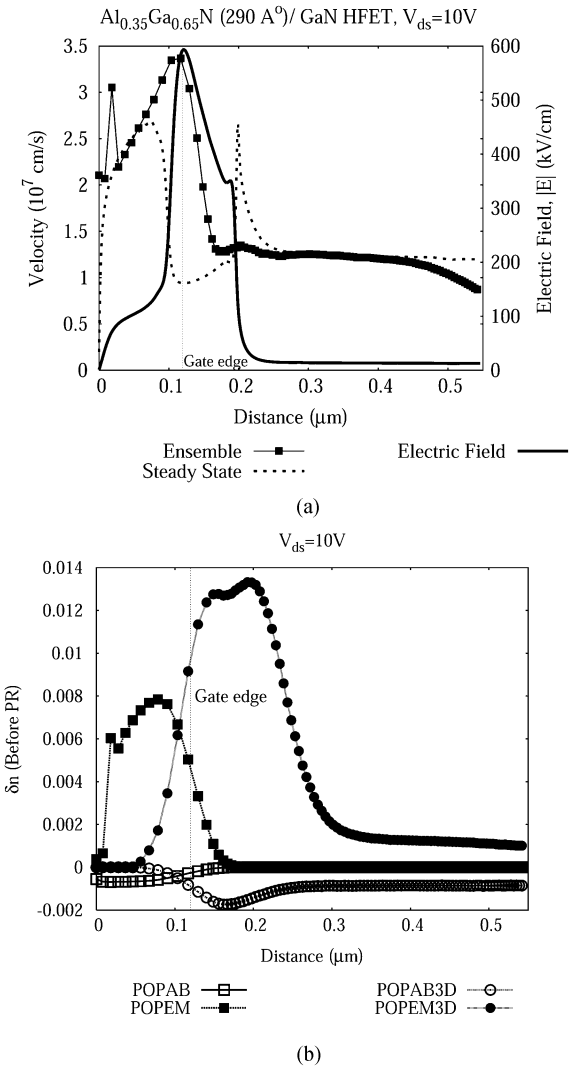

Fig. 7. $L_g = 0.12$ μm. (a) Ensemble averaged channel velocities, steady-state velocities and the electric field profile at $V_{\rm gs} = -2$ V. The Monte Carlo simulations are carried out over a region much larger than the gate area. The edge of the gate is indicated in the plots for reference. (b) Extra phonon population after one ensemble calculation, δn. The $-\mathbf{EM}$ labels correspond to emission processes, either in the two-dimensional confined portion of the channel or in the depleted part (three-dimensional), while $-\mathbf{AB}$ labels correspond to absorption processes.

with 200 000 electrons. It must be stressed that these ensemble calculations do *not* take the region of field reversal into account.

The region of field reversal presents an interesting issue. Since the electrons cannot drift through this region toward the drain, they have to diffuse (ignoring the opposing tendency of the locally reversed field to push the electrons toward the source). If the ensemble simulation is carried out for a smaller gate lengths ($L_g = 0.12, 0.25$ μm), we get the results shown in Figs. 4 and 5. As such, we would expect an increased influence of field reversal for the shorter gate lengths due to two causes: 1) The larger region of field reversal as a fraction of the gate length and the correspondingly shorter region over which the electron gains energy and 2) The increased opposing drift tendency in the region of reversal. As mentioned earlier, we ignore the latter effect in our treatment. It would serve to further enhance the delay time in the region as it reduces forward electron velocity.

If we ignore the region of field reversal and thermal effects, we can summarize the results obtained so far: there are varying degrees of overshoot for the three different gate lengths for higher drain biases. One may also notice the fact that the value of the peak electric field in the channel does not seem to scale simply with the gate length. This is a result of the nature of the device structure which is not self-aligned. Regions outside the gate region have a higher resistivity due to lower charge induced in these. For the lower drain bias, there does not appear to be any overshoot for the gate biases under consideration there.

It is also instructive to consider the effects of self-heating on the channel velocity profile. The channel velocity profiles for the same device structure with $L_g = 0.70$ μm, but at 400 K are shown in Fig. 10. In spite of the higher initial velocities, there is a visible reduction in the channel velocity due to greater randomization of carrier velocities in the channel, resulting in nearly equal channel exit velocities.

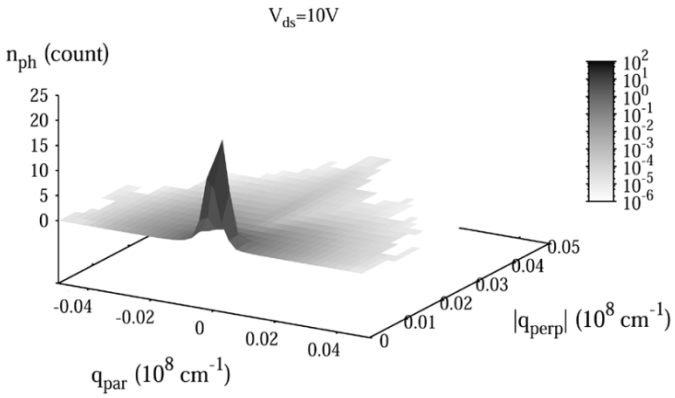

Fig. 8. $L_g = 0.12\ \mu$m. Momentum spectrum of ensemble averaged polar optical phonon count per electron for $V_{\rm gs} = -2$ V. As in Fig. 7, the Monte Carlo simulations are carried out over a region much larger than the gate area.

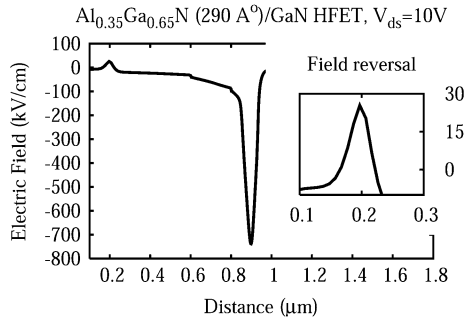

Fig. 9. $L_g = 0.70\ \mu$m. Electric field profile obtained through a finite element method for $V_{\rm gs} = -2$ V. The inset shows the region of field reversal in greater detail.

IV. Conclusion

In this paper, we have presented results for channel velocities for different gate lengths, for different biasing conditions and at two different temperatures. We have examined the effect of the nonequilibrium phonon occupations at 300 K and found that by itself, it has a negligible influence on the channel velocities. In absence of consideration of field reversal on the source end of the channel and self-heating effects, we find varying degrees of overshoot for all three gate lengths considered for $V_{\rm ds} = 10$ V. However, if we consider the results at lower drain biases (more likely to be employed for the shorter gate lengths), there is little or no overshoot at $V_{\rm ds} = 5$ V, a feature related to an order of magnitude higher scattering rates in III–V nitrides when compared to III–V arsenides.

The effect of self-heating arising from high-field transport can be seen to be leading to a faster suppression of the injection velocity (Fig. 10). The exact details of this effect are likely to be position dependent, and intimately related to the nature of transport in the region under consideration. While such effects might arise in part from relatively large numbers of phonons emitted just outside the gate on the drain side (as borne out by Fig. 7), it does not appear that the phonons emitted in regions far removed from the drain end of the gate region (GD) would lead to significant self-heating effects.

As discussed earlier, suppression of velocity overshoot due to diffusive transport through the field reversal region is expected to be more pronounced for smaller channel lengths. The

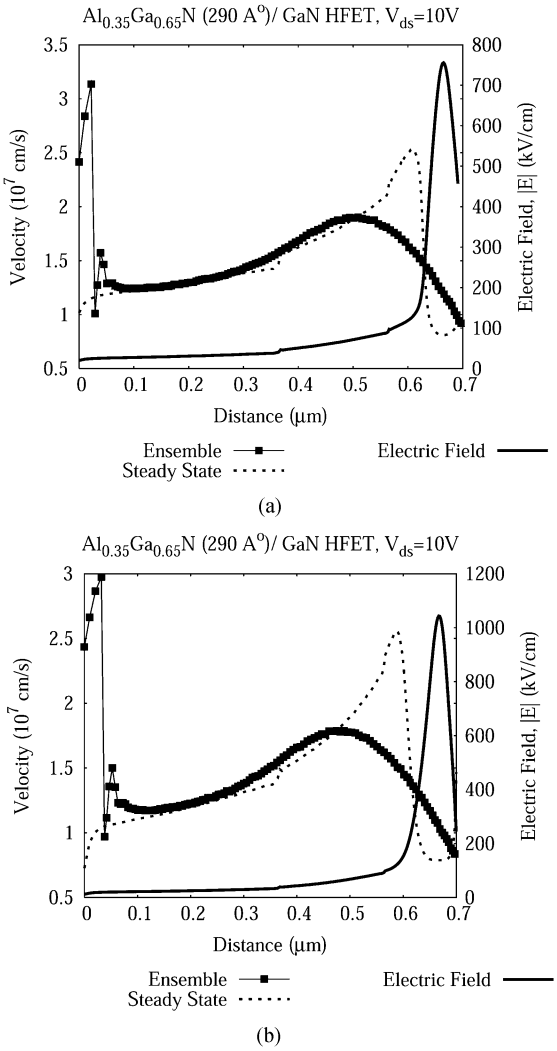

Fig. 10. Electric field and channel velocity profile results for $L_g = 0.70\ \mu$m at 400 K for (a) $V_{\rm gs} = -2$ V and (b) $V_{\rm gs} = -4$ V.

presence of this field reversal region may be directly related to the fact that the device structure is not self-aligned. The structure considered (Fig. 1) is not self-aligned. Reduction of the gate-source and gate-drain distance would reduce the physical extent of the field reversal region and result in a weaker field reversal overall. Use of a self-aligned structure, would not only reduce the length of the field reversal region but also enhance the electric field in the channel by reducing the relatively long regions of resistive drops between the source contact and the gate and the gate and the drain contact.

It may also be noted that the results that ignore the presence of the field-reversal region and the effect of transport in the gate drain region (unlike Fig. 7), correspond physically to a self-aligned structure. Thus, results shown in Figs. 3, 4, 5, 6, and 10 represent an upper limit on device performance, imposed by high scattering rates in this system.

Other researchers have attempted to explain the lack of observed overshoot on the basis of generation of nonequilibrium or *hot* phonons [13]–[15]. In this paper, we have presented a comparative study of the effects of the nonequilibrium phonons emitted in the channel (and possible self-heating), presence of

regions of field reversal, and high scattering rates, and as a consequence, their implication for the prospect of velocity overshoot. In a forthcoming publication, we will be addressing the effect of these factors on the saturation of transconductance (g_m) in III–V nitride HFETs.

REFERENCES

[1] S. Babiker, N. Cameron, A. Asenov, and S. P. Beaumont, "New evidence for velocity overshoot in a 200 nm pseudomorphic HEMT," *Micro. J.*, no. 8, pp. 785–793, 1996.

[2] M. Wraback, H. Shen, J. C. Carrano, C. J. Collins, J. C. Campbell, R. D. Dupuis, M. J. Schurman, and I. T. Ferguson, "Time-resolved electroabsorption measurement of the transient electron velocity overshoot in GaN," *Appl. Phys. Lett.*, vol. 79, no. 9, pp. 1303–1305, 2001.

[3] H. K. Gummel, "A self-consistent iterative scheme for one-dimensional steady-state transistor calculations," *IEEE Trans. Electron. Devices*, vol. ED-11, pp. 455–465, 1964.

[4] Y. Zhang and J. Singh, "Charge control and mobility studies for an AlGaN–GaN high electron mobility transistor," *J. Appl. Phys.*, vol. 85, no. 1, pp. 587–594, 1999.

[5] M. Singh, Y. Zhang, J. Singh, and U. Mishra, "Examination of tunnel junctions in the AlGaN–GaN system: Consequences of polarization charge," *Appl. Phys. Lett.*, vol. 77, no. 12, pp. 1867–1869, 2000.

[6] M. Singh and J. Singh, "Design of high electron mobility devices with composite nitride channels," *J. Appl. Phys.*, vol. 94, no. 4, pp. 2498–2506, Aug. 2003.

[7] T.-H. Yu and K. F. Brennan, "Theoretical study of a GaN-AlGaN high electron mobility transistor including a nonlinear polarization model," *IEEE Trans. Electron. Devices*, vol. 50, no. 2, pp. 315–323, Feb. 2003.

[8] J. M. Barker, D. K. Ferry, S. M. Goodnick, D. D. Koleske, A. Allerman, and R. J. Shul, "High field transport in GaN/AlGaN heterostructures," *J. Vac. Sci. Technol. B, Condens. Matter*, vol. 22, no. 4, pp. 2045–2050, 2004.

[9] M. Farahmand, C. Garetto, E. Bellotti, K. J. Brennan, M. Goano, E. Ghilino, G. Ghione, J. D. Albrecht, and P. P. Ruden, "Monte Carlo simulation of electron transport in the III-nitride Wurtzite phase materials system: Binaries and ternaries," *IEEE Trans. Electron. Devices*, vol. 48, no. 3, pp. 535–542, Mar. 2001.

[10] R. Li, S. J. Cai, L. Wong, Y. Chen, K. L. Wang, R. P. Smith, S. C. Martin, K. S. Boutros, and J. M. Redwing, "An $Al_{0.3}Ga_{0.7}N$/GaN undoped channel heterostructure field effect transistor with F_{max} of 107 GHz," *IEEE Electron Device Lett.*, vol. 20, no. 7, pp. 323–325, Jul. 1999.

[11] E. M. Chumbes, A. T. Schremer, J. A. Smart, Y. Wang, N. C. MacDonald, D. Hogue, J. J. Komiak, S. J. Lichwalla, R. E. Leoni III, and J. R. Shealy, "AlGaN/GaN high electron mobility transistors on Si(111) substrates," *IEEE Trans. Electron Devices*, vol. 48, no. 3, pp. 420–426, Mar. 2001.

[12] W. Lu, V. Kumar, E. L. Piner, and I. Adesida, "DC, RF, and microwave noise performance of AlGaN-GaN field effect transistors dependence of aluminum concentration," *IEEE Trans. Electron Devices*, vol. 50, no. 4, pp. 1069–1074, Apr. 2003.

[13] A. Matulionis, J. Liberis, L. Ardaravicius, J. Smart, D. Pavlidis, S. Hubbard, and L. F. Eastman, "Hot-phonon limited electron energy relaxation in AlN/GaN," *Int. J. High Speed Electron. Systems*, no. 2, pp. 459–468, 2002.

[14] L. Ardaravicius, A. Matulionis, J. Liberis, O. Kiprijanovic, M. Ramonas, L. F. Eastman, J. R. Shealy, and A. Vertiatchikh, "Electron drift velocity in AlGaN–GaN channel at high electric fields," *Appl. Phys. Lett.*, vol. 83, no. 19, pp. 4038–4040, 2003.

[15] A. Matulionis, J. Liberis, L. Ardaravicius, L. F. Eastman, J. R. Shealy, and A. Vertiatchikh, "Hot-phonon lifetime in AlGaN/GaN at a high lattice temperature," *Semicond. Sci. Technol.*, vol. 19, no. 4, pp. S421–S423, 2004.

Madhusudan Singh (S'99) received the M.Sc. (Integrated) degree in physics from the Indian Institute of Technology, Kanpur, India, in 1999. He received the M.S. degrees in electrical engineering and mathematics from the University of Michigan, Ann Arbor, in 2003, where he is currently pursuing the Ph.D. degree in electrical engineering at the Department of Electrical Engineering and Computer Science.

His current research includes theoretical studies of vertical and parallel transport in III–V nitride heterostructures, ferroelectrics, and organic semiconductors.

Yuh-Renn Wu (S'03) received the B.S. degree in physics and the M.S. degree in communication engineering from National Taiwan University, Taipei, Taiwan, R.O.C., in 1998 and 2000, respectively. He is currently pursuing the Ph.D. degree in electrical engineering at the Department of Electrical Engineering and Computer Science, University of Michigan, Ann Arbor.

His current research includes theoretical studies of vertical and parallel transport in III–V nitride heterostructures, ferroelectrics, and opto-electronic devices.

Jasprit Singh received the Ph.D. degree in solid-state physics from the University of Chicago, Chicago, IL, in 1980, where he worked in the area of disordered semiconductors.

He then spent three years at the University of Southern California, two years at Wright-Patterson AFB, Ohio, and has been at the University of Michigan, Ann Arbor, since 1985. His area of research is physics and design of semiconductor heterostructure devices. He has worked on electronic and opto-electronic devices based on traditional III–V materials, HgCdTe, SiGe, and the nitrides. His current research is exploiting ferroelectric materials within conventional semiconductor devices. His recent books are: *Modern Physics for Engineers*, (New York, NY: Wiley Interscience, 1999) and *Semiconductor Devices: Basic Principles*, (New York, NY: Wiley , 2001).